

Post-print dell'articolo: *Reliability of water content estimation by profile probe and its effect on slope stability.*

In accordo con le politiche editoriali della rivista si riporta di seguito il link della pubblicazione definitiva con il doi.

<https://link.springer.com/article/10.1007/s10346-017-0895-7>

1 **Reliability of water content estimation by profile probe and its effect on slope stability**

2
3 Di Matteo, Lucio^{1*}; Pauselli, Cristina²; Valigi, Daniela³; Ercoli, Maurizio⁴; Rossi, Mauro⁵,
4 Guerra, Giacomo⁶; Cambi, Costanza⁷; Ricco, Remo⁸; Vinti, Giuseppe⁹

5
6 ^{1*}*Corresponding author*: Department of Physics and Geology, University of Perugia, Via A.
7 Pascoli snc, 06123 Perugia (Italy), Phone +39 0755849694, Fax +39 0755840302, e-mail:
8 lucio.dimatteo@unipg.it; orcid.org/0000-0002-3352-3858.

9 ² Department of Physics and Geology, University of Perugia, Via A. Pascoli snc, 06123
10 Perugia (Italy), e-mail: cristina.pauselli@unipg.it; orcid.org/0000-0002-5507-8003.

11 ³ Department of Physics and Geology, University of Perugia, Via A. Pascoli snc, 06123
12 Perugia (Italy), e-mail: daniela.valigi@unipg.it; orcid.org/0000-0002-2256-251X.

13 ⁴ Department of Physics and Geology, University of Perugia, Via A. Pascoli snc, 06123
14 Perugia (Italy), e-mail: maurizio.ercoli@unipg.it; orcid.org/0000-0001-6062-9175.

15 ⁵ CNR IRPI, via Madonna Alta 126, 06128 Perugia (Italy), e-mail: mauro.rossi@irpi.cnr.it;
16 orcid.org/0000-0002-0252-4321.

17 ⁶ Department of Physics and Geology, University of Perugia, Via A. Pascoli snc, 06123
18 Perugia (Italy), e-mail: guerragiacomio51@gmail.com;

19 ⁷ Department of Physics and Geology, University of Perugia, Via A. Pascoli snc, 06123
20 Perugia (Italy), e-mail: costanza.cambi@unipg.it; orcid.org/0000-0002-7343-469X.

21 ⁸ Istituto Sperimentale per l'Edilizia (ISTEDIL), Loc. S. Andrea delle Fratte, 06132 Perugia
22 (Italy), e-mail: r.ricco@istedil.com;

23 ⁹ Department of Physics and Geology, University of Perugia, Via A. Pascoli snc, 06123
24 Perugia (Italy), e-mail: giuseppe.vinti@unipg.it;

25 **Abstract**

26 Shallow landslide failures are distributed worldwide and cause economic losses and fatalities.
27 A proper evaluation of the possible occurrence of shallow landslides requires reliable
28 characterization of water content. Volumetric water content (θ) is commonly estimated using
29 dielectric sensors, which use manufacturers' calibration curves developed for specific soil
30 types. In this study, we present the experimental results achieved during a laboratory
31 calibration of a capacitance probe (PR2/6 probe), tested on two sandy soils widely
32 outcropping in Central Italy. The proposed equations demonstrate a more reliable estimation
33 of θ with respect to the generalized soil equation provided by the manufacturer, which
34 overestimates θ by up to 10 percentage points. Such overestimation could affect the
35 evaluation of suction stress in partially saturated shallow soils affecting the slope stability
36 analysis. Although the use of θ from correct calibration equations provides less precautionary
37 factor of safety values, a reliable evaluation of the soil moisture condition is fundamental
38 when mapping and predicting the spatial and temporal occurrence of shallow landslides. The
39 use of the PR2/6 probe with the appropriate soil calibration equations in early warning
40 monitoring systems will provide a more reliable forecast, minimizing the number of false
41 alarms.

42 **Keywords:** landslides, water content, PR2/6 probe, sandy soils, suction stress.

43

44

45

46

47

48 **1. Introduction**

49 Landslide susceptibility assessments and slope stability analysis are affected by
50 measurements, mapping, modelling errors and uncertainties (Ang and Tang, 1984; Baecher
51 and Christian, 2003; Guzzetti et al., 2006; Rossi et al., 2010; Di Matteo et al., 2013; Jiang et
52 al., 2015; Rossi and Reichenbach, 2016; Rossi et al., 2017). The understanding and
53 forecasting of geohydrologic phenomena require a reliable estimation of the water content of
54 unsaturated soils (Babu and Murthy, 2005; Zhang et al., 2011; Sahis et al., 2014). This is
55 particularly relevant to shallow landslides, which generally involve small volumes of soil.

56 Although the water content by the gravimetric method (θ_g – eq. 1) is the standard to measure
57 the water content of porous media and used to compare results from other methods (Walker
58 et al., 2004), the volumetric water content (θ – eq. 2) is largely used in place of θ_g ,
59 particularly in slope stability analysis and numerical landslide modelling. θ can be expressed
60 in terms of θ_g by knowing the dry unit weight of soil γ_d , eq. 3.

61

62 $\theta_g = \frac{M_w}{M_s}$ 1); $\theta = \frac{V_w}{V_T}$ 2); $\theta = \theta_g \cdot \frac{\gamma_d}{\gamma_w}$ 3)

63 where:

64 M_w = mass of water (kg);

65 M_s = mass of solids (kg);

66 V_w = volume of water (m³);

67 V_T = volume of soil sample (m³);

68 γ_d = dry unit weight of soil (kN/m³);

69 γ_w = unit weight of water (kN/m³).

70

71 Unlike the estimation of θ , the gravimetric method is time-consuming, requires the soil
72 sampling (destructive method), and does not allow a continuous space-time monitoring of the
73 water content (Rudnick et al., 2015). The latter poses important limitations when distributed
74 modelling approaches are used, which require the knowledge of the variations of the water
75 content in space and time. According to Chae et al. (2014), the response of θ to rainfall
76 events is more immediate than pore water pressure changes. This indicates that observation
77 of θ and its changes over time at shallow soil depths may be relevant for landslides
78 monitoring. Among the field sensors for near-real-time landslide monitoring, dielectric soil-
79 moisture probes are used in unsaturated soil conditions (Reid et al., 2008). These probes
80 included Time Domain Reflectometers (TDR), Frequency Domain Reflectometers (FDR)
81 and Capacitance Probes (CP). The reliability of indirect measurements by soil-moisture
82 probes is strongly affected by the calibration procedure used for water content estimation.
83 The use of equations provided by the manufacturer could lead to unreliable estimations of the
84 water content, thus to improve the performance of sensors, soil-calibrations are required
85 (Evelt et al., 2006; Bogaen et al., 2007; Robinson et al., 2008; Mazahrih et al., 2008).
86 According to Kizito et al. (2008), soil water monitoring devices require a laboratory
87 evaluation and calibration for a range of soil types prior to field deployment. Laboratory soil-
88 column experiments can be useful to calibrate the equipment or to compare the performance
89 of different instruments on different soil types under controlled conditions (Paltineanu and
90 Starr, 1997; Baumardth et al., 2000; Huang et al., 2004; Irmak and Irmak 2005; Polyakov et
91 al., 2005; Evelt et al., 2006; Kim et al., 2008). As reported by Irmak and Irmak (2005), few
92 studies have evaluated the performance of FDR and CP in coarse-textured soils under

93 controlled experimental conditions. This critical aspect holds also for other hydrological
94 applications, such as satellite soil moisture products and/or the use of infiltration and surface
95 runoff models, which require reliable in situ soil moisture data (Brocca et al., 2011;
96 Morbidelli et al., 2012).

97 Quantifying uncertainty of soil variables, such as θ , is necessary to evaluate hydrologically-
98 driven processes. The investigation of the effects of non-specific soil equations for θ
99 estimation on the suction stress is of interest, being the latter an important component of
100 slope stability analysis of unsaturated soils. The present work aims to calibrate the PR2/6
101 profile probe (capacitance probe, Delta-T Devices) at laboratory scale on sandy soils. We
102 quantify and discuss these aspects taking as reference two soils from Central Italy. Specific
103 calibration equations to estimate θ in sandy soils are presented and compared with the default
104 calibration equation for mineral soils provided by the manufacturer and with other equations
105 available in the literature.

106

107 **2. Material and methods**

108 **2.1 Study area**

109 Two sampling sites characterized by sandy deposits widely outcropping in Central Italy were
110 selected: the alluvial plains of (A) Nera and (B) Tiber rivers (Fig. 1). The mineralogy of the
111 two soils is different: soil S_A (Conca Ternana alluvial plain) is mainly composed by
112 carbonates, while soil S_B (Tiber River alluvial plain) is a typical flyschoid sand being
113 composed by micas, pyrite, and quartz. The two sites have been chosen because they are
114 easily accessible to soil sampling and the mineralogical characteristics of the materials can be
115 considered as representative of recent and ancient fluvial-lacustrine deposits (Fig. 1) widely

116 outcropping along alluvial plains and hill slopes in Umbria Region and in other places in
117 Central Italy.

118 **FIG. 1**

119

120 **2.2 Soil characteristics**

121 For each soil, particle size distribution (ASTM D422-631998), specific gravity G_s (CEN
122 ISO/TS 17892-3 2004), Atterberg limits (CEN ISO/TS 17892-12 2004), compaction
123 properties (standard Proctor test, ASTM D698 - 12e2), and organic matter (ASTM D2974 -
124 14) were determined in laboratory.

125 Table 1 summarizes the main geotechnical properties of soils. Compaction behaviour of Soil
126 S_A is typical of poorly-graded sands (coefficient of uniformity, $C_u = 3$): the presence of large
127 amounts of voids leads to lower Maximum Dry Density (MDD) with respect to Soil S_B
128 which contains about 18% of fines (Table 1).

129

130 **TABLE 1**

131 **2.3 Experimental setup**

132 Laboratory investigations were carried out in order to determine the specific soil equations to
133 estimate θ of the two selected sandy soils. Soils were mixed with tap water and left for 24
134 hours to moisten at controlled temperature conditions ($T = 22 \pm 1$ °C). The procedure was
135 repeated several times in order to obtain soils with different θ_g values. Then, the soils were
136 placed and manually compacted in a cylindrical PVC container (soil column, diameter 0.50
137 m and height 1.30 m, Fig. 2a). Compaction was conducted repeatedly by dropping a
138 cylindrical hammer (used to drive the core cutter system into the soil as standardized by BS
139 1377-9:1990, mass = 13.5 kg; diameter = 0.15 m) from a height of about 0.20 m. In order to

140 make the procedure repeatable, approximately 0.10 m of damp sand was laid and compacted
 141 using 25 blows, as for the standard Proctor test (Fig. 2b). The compaction procedure allowed
 142 analysis of the soils over a wide range of water content and degree of saturation values.
 143 Thanks to the compaction procedure, the water content was homogeneously distributed in
 144 each soil column (this was verified on soils sampled at different depths). The compaction
 145 was carried out all around an access tube, placed at the centre of the soil column. The profile
 146 probe PR2/6 (Delta-T Devices, Cambridge, UK) was placed in the access tube allowing the
 147 estimation of θ at different depths (0.10, 0.20, 0.30, 0.40, 0.60, and 1.00 m) by measuring the
 148 dielectric constant (ϵ) of the damp soil. In the PR2/6 probe, a signal of 100 MHz is applied to
 149 six pairs of stainless steel rings, which transmits an electromagnetic field extending about
 150 0.10 m into the soil (Fig. 2a). The change in the circuit output (in Volts - V) is related to the
 151 square root of soil permittivity ($\sqrt{\epsilon}$) by a sixth-order polynomial fit (eq. 4, Delta-T Devices
 152 Ltd, 2016). Topp et al. (1980) showed that there is a simple linear relationship between the
 153 complex refractive index (similar to $\sqrt{\epsilon}$) and θ . The generalized equation given by the
 154 manufacturer for mineral soils, meant as generic soils having low organic matter, is shown in
 155 eq. 5. Information on characteristics of mineral soils (are available from Van Bavel and
 156 Nichols (2002) and Delta-T Devices Ltd (2016). The default parameters a_0 (soil offset) and a_1
 157 (slope) suggested by the manufacturer for mineral soils (Delta-T Devices Ltd, 2016) are 1.6
 158 and 8.4.

$$159 \quad \sqrt{\epsilon} = 1.125 - 5.53 \cdot V + 61.17 \cdot V^2 - 234.42 \cdot V^3 + 413.56 \cdot V^4 - 356.68 \cdot V^5 + 121.53 \cdot V^6 \quad 4)$$

$$160 \quad \sqrt{\epsilon} = a_0 + a_1 \cdot \theta = 1.6 + 8.4 \cdot \theta \quad 5)$$

161 The permittivity of the soil measured by dielectric sensors (ϵ) is given by the sum of soil real
 162 (ϵ') and imaginary (ϵ'' , dielectric loss) permittivity (eq. 6), where j is the imaginary constant,
 163 which is equal to $\sqrt{-1}$ (Robinson et al., 1999):

164 $\varepsilon = \varepsilon' + j \cdot \varepsilon''$ 6)

165 Muñoz–Carpena et al. (2005) state that, soil temperature (T), salinity of the effluent pore
166 fluid, and operating frequency affect ε'' . According to Scudiero et al. (2012), the contribution
167 of ε'' in saline soils cannot be ignored especially when sensors working at low frequencies
168 (<1 GHz) are used. Laboratory experiments using the 100 MHz PR2/6 were carried out with
169 tap water as pore fluid (Electrical Conductivity, EC = 400 $\mu\text{S}/\text{cm}$). Additionally, EC of the
170 water from saturated soil-pastes was determined. The soil-paste was saturated by adding
171 distilled water to 200 g of air dry soil and left 24 hours to permit the soil to fully imbibe the
172 water and the readily soluble salts to fully dissolve (Rhoades et al., 1999). The EC values of
173 the effluent fluid were then measured resulting 416 $\mu\text{S}/\text{cm}$ for soil S_A and 444 $\mu\text{S}/\text{cm}$ for soil
174 S_B . As investigated by Rüdiger et al. (2010) and Sevostianova et al. (2015) - depending on
175 the dielectric sensor used - the effect of pore water salinity on θ is appreciable for values
176 higher than 1500-5000 $\mu\text{S}/\text{cm}$. In this study, the values of salinity of the effluent pore fluid
177 are an order of magnitude lower, thus the effect of salinity on PR2/6 output is negligible.
178 During the experiments, two series of readings, of three measurements each, were made by
179 rotating the PR2/6 profile probe of 120° . This allowed to obtain by eq. 4 an average value of
180 $\sqrt{\varepsilon}$. In order to obtain representative measures of θ_g and γ_d – necessary for the computation of
181 θ with the eq. 3 – three soil samples were collected within the soil-column around the PR2/6
182 access tube. For the calibration purposes, all the measurements ($\sqrt{\varepsilon}$ with PR2/6 probe and θ
183 from soil sampling) are taken at a depth of 0.4 m (Fig. 2a, 2b). This procedure was applied to
184 both soils, S_A and S_B , taking into account several degree of saturation (S_r) from “quasi” dry
185 ($S_r = 5\%$) to wet ($S_r = 92\%$).

186

187 **3. Results**

188 The calibration procedure required the comparison of the dielectric properties of the damp
189 soil ($\sqrt{\epsilon}$), measured by the PR2/6 profile probe, and θ from soil sampling. Figure 3 shows the
190 plot of experimental data for soils S_A and S_B (θ vs $\sqrt{\epsilon}$): regression lines of these soils allowed
191 to obtain the specific parameters (a_0 and a_1) for both soils (eqs. 7 and 8).

$$192 \quad \sqrt{\epsilon} = a_0 + a_1 \cdot \theta = 1.7 + 9.5 \cdot \theta \quad (S_A, R^2 = 0.995) \quad 7)$$

$$193 \quad \sqrt{\epsilon} = a_0 + a_1 \cdot \theta = 1.9 + 10.6 \cdot \theta \quad (S_B, R^2 = 0.997) \quad 8)$$

194 The two equations differ from that suggested for mineral soils by the manufacturer (eq. 5).
195 The use of eq. 5 produces an overestimation of θ , particularly appreciable for $\sqrt{\epsilon}$ higher than
196 3. As an example, for $\sqrt{\epsilon} = 4.5$, the eq. 5 overestimates θ values of about 5 and 10 percentage
197 points for soil S_A (calcareous sand) and soil S_B (flyschoid sand), respectively.

198 The comparison with literature data indicated that the calibration curve for calcareous sands
199 (soil S_A) could also be used for quartz sands (Fig. 3). Comparison has been carried out with
200 the calibration line (θ vs $\sqrt{\epsilon}$) of Theta probe device presented by Robinson et al. (1999). The
201 principles of Theta Probe are similar to those of profile probes, such as the PR2/6 probe (cf.
202 Cooper, 2001). Both devices measure, at the same frequency of 100 MHz, the same physical
203 parameter, the dielectric constant ($\sqrt{\epsilon}$).

204 **FIG. 2**

205 **FIG. 3**

206

207 **4. Discussion**

208 Erroneous estimate of θ by PR2/6 profile probe may derive from the use of manufacturer's
209 equation in place of soil-specific calibration equations. Reliable θ values are fundamental for
210 a proper estimation of the suction stress (σ^s). According to Lu and Likos (2004), suction
211 stress can be expressed in terms of normalized volumetric water content (eq. 9).

212
$$\sigma^s = -\frac{\theta - \theta_r}{\theta_s - \theta_r} \cdot (u_a - u_w) \quad 9)$$

213 Where:

214 σ^s = suction stress (kN/m²);

215 θ = volumetric water content (dimensionless);

216 θ_r = residual volumetric water content (dimensionless);

217 θ_s = saturated volumetric water content (dimensionless);

218 u_a = pore air pressure (kN/m²);

219 u_w = pore water pressure (kN/m²);

220 $u_a - u_w$ = matrix suction (kN/m²);

221

222 The Soil Water Characteristics software (version 6.02.75) available from
223 <https://hrsl.ba.ars.usda.gov/soilwater/Index.htm> is a useful tool for hydrological soil
224 properties estimations. The software allows the estimation of soil water tension, conductivity
225 and water holding capability based on the soil physical properties of texture, organic matter,
226 gravel, salinity, and compaction (Saxton and Rawls, 2006). Based on soil physical properties
227 of both soils summarized in Table 1, the model developed by Saxton et al. (1986),
228 implemented in the software, allowed the estimation of the Soil Water Characteristic Curve
229 (SWCC). SWCC parameters (θ_r and θ_s) are related to the matrix suction ($u_a - u_w$) by the
230 volumetric water content (θ). Table 2 summarizes the main SWCC parameters and suction
231 stress values for θ values calculated by the manufacturer equation (eq. 5) and the specific-soil
232 calibration curves provided by the present work (eqs. 7 and 8). In the calculation a $\sqrt{\epsilon}$ by
233 PR2/6 equal to 4.5 was used, corresponding to S_r higher than 50%, regardless the calibration
234 lines used (Fig. 4).

235

TABLE 2

236

FIG. 4

237

238 As reported by Lu and Likos (2004, 2006), the generalized effective stress that unifies both
239 saturated and unsaturated conditions can be expressed by eq. 10, where σ is the total stress.

$$240 \quad \sigma' = (\sigma - u_a) - \sigma^s \quad 10)$$

241 The suction stress is an important component in evaluating the Factor of Safety (FS) for
242 shallow slope failures occurring within the vadose zone under partially saturated soil
243 conditions (Wolle and Hachich, 1989; de Campos et al., 1991; Godt et al., 2007; Lu and
244 Godt, 2008). For simplicity and wide usage, the limit equilibrium method can be used to
245 evaluate the stability of landslides with longitudinal dimensions much larger than failure
246 plane depth (Doglioni et al., 2013). For uniform homogeneous and unlimited slopes with
247 inclination β characterized by cohesionless soil and groundwater table parallel to the slope,
248 FS can be calculated using eq. 11 (Lu and Godt, 2008). Such approach account for θ
249 variations in the unsaturated zone.

$$250 \quad FS = \frac{\tan \phi'}{\tan \beta} - \frac{\sigma^s}{\gamma \cdot H_{ss}} \cdot (\tan \beta + \cot \beta) \cdot \tan \phi' \quad 11)$$

251 where:

252 ϕ' = friction angle ($^\circ$);

253 β = slope angle ($^\circ$);

254 γ = unit weight of soil (kN/m^3);

255 H_{ss} = depth of sliding surface (m).

256

257 The findings of the present study show how the use of calibration equations allows a proper
258 estimation of θ and then σ^s . According to eqs. 9, the overestimate of θ from manufacturer's
259 equation results in an error of suction stress by up to about 2.7 kPa. As a consequence, the
260 effective stress (σ' , eq. 10) reduces. Referring to eq. 11 and assuming constant values of ϕ' ,
261 β , and γ , for a given depth of sliding surface (H_{ss}) this error also causes inevitably a reduction
262 of the FS value. As an example, Fig. 5 shows the differences when calculating FS at two
263 depth of sliding surface ($H_{ss} = 0.6$ and 1.0 m) considering the error of θ and σ^s estimation for
264 the different soils (Table 2) and assuming ϕ' equal to 34° (value suggested by Hoek and Bray
265 1981 for homogeneous sands having γ_d of 14.0 kN/m³). Such FS differences due to the use of
266 inappropriate PR2 probe empirical equations (θ vs $\sqrt{\epsilon}$) may affect the modelling of spatial
267 and temporal occurrence of landslides.

268 FIG. 5

269

270 5. Conclusions

271 The work discusses the reliability of volumetric water content estimation using the PR2/6
272 probe on two sandy soils widely outcropping in Central Italy and its effects on suction stress
273 estimation and slope stability analysis. The results confirm that - in order to have reliable
274 measurements - specific soil calibration equations are required. The use of manufacturer's
275 equation brings to errors in θ estimation, which inevitably affect the evaluation of S_r for the
276 unsaturated region (by up to 22 percentage points for a given dry unit weight). Overall, the
277 results here presented indicate that the overestimation of θ values decreases the effective
278 stress and hence reduce the shear strength, which causes a lower FS. In other words the
279 overestimation of θ produces more precautionary (i.e., lower) FS values. Since the θ time-
280 space evolution of the unsaturated region influences the initiation of shallow landslides, the

281 use of reliable θ values is fundamental to model their spatial and temporal occurrence (Glade
282 et al., 2000; Alvioli et al., 2014; Raia et al., 2014; Cullen et al., 2016). The use of such probe
283 with the appropriate soil calibration equations in early warning monitoring systems will
284 provide more reliable forecast, minimizing the number of false alarms.

285 Given these results, further studies devoted to the calibration of dielectric sensors on other
286 types of soil should be carried out. In addition, the identification of landslide forecasting and
287 susceptibility modelling approaches that accounts for the uncertainty and reliability of water
288 related parameters should be encouraged.

289

290 **Acknowledgments**

291 The geotechnical analyses were performed in the Laboratorio di Geologia Applicata of the
292 University of Perugia funded in the framework of the “*Ricerca di base 2014 Project –*
293 *DIMBASE14*”. The authors are grateful for the technical support provided by Laboratorio
294 Preparazione Rocce e Sezioni Sottili of the University of Perugia.

295

296 **References**

297 Alvioli M, Guzzetti F, Rossi M (2014) Scaling properties of rainfall induced landslides
298 predicted by a physically based model. *Geomorphology* 213:38-47.
299 <https://doi.org/10.1016/j.geomorph.2013.12.039>.

300 Ang AHS, Tang WH (1984) Probability concepts in engineering planning and design.
301 Volume II - decision, risk and reliability. Wiley, New York, 562 pp.

302 Babu GLS, Murthy DSN (2005) Reliability analysis of unsaturated soil slopes. *J Geotech*
303 *Geoenviron Eng* 131:1423–1428. [https://doi.org/10.1061/\(ASCE\)1090-](https://doi.org/10.1061/(ASCE)1090-0241(2005)131:11(1423)#sthash.VhJP7Gcy.dpuf)
304 [0241\(2005\)131:11\(1423\)#sthash.VhJP7Gcy.dpuf](https://doi.org/10.1061/(ASCE)1090-0241(2005)131:11(1423)#sthash.VhJP7Gcy.dpuf)

305 Baecher GB, Christian JT (2003) Reliability and statistics in geotechnical engineering.
306 Wiley, London.

307 Baumardth RL, Lascano LJ, Evett SR (2000) Soil material, temperature and salinity effects
308 on calibration of multisensor capacitance probes. *Soil Sci Soc Am J* 64:1940-1946.

309 Bogena HR, Huisman JA, Oberdörster C, Vereecken H (2007) Evaluation of a low-cost soil
310 water content sensor for wireless network applications. *J Hydrol* 344:32–42.
311 <https://doi.org/10.1016/j.jhydrol.2007.06.032>

312 Brocca L, Hasenauer S, Lacava T, Melone F, Moramarco T, Wagner W, Dorigo W, Matgen
313 P, Martínez-Fernández J, Llorens P, Latron J, Martin C, Bittelli M (2011) Soil moisture
314 estimation through ASCAT and AMSR-E sensors: An intercomparison and validation
315 study across Europe. *Remote Sens Environ* 115(12):3390–3408.
316 <https://doi.org/10.1016/j.rse.2011.08.003>.

317 Chae B-J, Choi J, Seo Y-K (2014) Suggestion of a Landslide Early Warning Method Using a
318 Gradient of Volumetric Water Content. In: K. Sassa et al (eds), *Landslide Science for a
319 Safer Geoenvironment– Volume 2: Methods of Landslide Studies*. Springer International
320 Publishing, Switzerland, pp. 545-550.

321 Cooper DD (2001) *Soil water measurement: A practical handbook*. Wiley Blackwell, 368 pp.

322 Cullen CA, Al-Suhili R, Khanbilvardi R (2016) Guidance Index for Shallow Landslide
323 Hazard Analysis. *Remote Sensing* 8: 866-883. <https://doi.org/10.3390/rs8100866>.

324 de Campos TMP, Andrade MHN, Vargas Jr EA (1991) Unsaturated colluvium over rock
325 slide in a forested site in Rio de Janeiro, Brazil, in *Proc. 6th Int. Symp. on Landslides*,
326 Christchurch New Zealand, pp. 1357– 1364, Balkema, Rotterdam, Netherlands.

327 Delta-T Devices Ltd (2016). User Manual for the Profile Probe, typePR2. 48 pp. Available at
328 https://www.delta-t.co.uk/wp-content/uploads/2017/02/PR2_user_manual_version_5.0.pdf.
329 Last accessed, July 31th, 2017.

330 Di Matteo L, Valigi D, Ricco R (2013) Laboratory shear strength parameters of cohesive
331 soils: variability and potential effects on slope stability. *Bull Eng Geol Environ* 72(1): 101–
332 106. <https://doi.org/10.1007/s10064-013-0459-6>.

333 Doglioni A, Galeandro A, Simeone V (2013) Lateral strength and critical depth in infinite
334 slope stability analysis. *Int J Numer Anal Meth Geomech* 38:1–19.
335 <https://doi.org/10.1002/nag.2190>.

336 Evett SR, Tolk JA, Howell TA (2006) Soil profile water content determination: sensor
337 accuracy, axial response, calibration, temperature dependence, and precision. *Vadose Zone*
338 *J* 5:894–907. <https://doi.org/10.2136/vzj2005.0149>.

339 Glade T, Crozier MJ, Smith P (2000) Applying probability determination to refine
340 landslide-triggering rainfall thresholds using an empirical “Antecedent Daily Rainfall
341 Model”. *Pure Appl Geophys* 157(6/8):1059–1079. <https://doi.org/10.1007/s000240050017>.

342 Godt JW, Baum RL, McKenna JP (2007) Vadose-zone response to rainfall leading to
343 shallow landslide initiation on the Puget Sound bluffs, Washington. *Geol. Soc. Am. Abstr.*
344 *Programs*, 36(6): 362.

345 Guzzetti F, Reichenbach P, Ardizzone F, Cardinali M, Galli M (2006) Estimating the quality
346 of landslide susceptibility models. *Geomorphology* 81(1):166-184.
347 <https://doi.org/10.1016/j.geomorph.2006.04.007>.

348 Hoek E, Bray J (1981) *Rock Slope Engineering*. Revised 3rd Edition, The Institution of
349 Mining and Metallurgy, London, 341-351.

350 Huang Q, Akinremi OO, Sri Rajan R, Bullock P (2004) Laboratory and field evaluation of
351 five soil water sensors. *Can J Soil Sci* 84:431–438. <https://doi.org/10.4141/S03-097>.

352 Irmak S, Irmak A (2005) Performance of frequency-domain reflectometer, capacitance, and
353 psuedo-transit time-based soil water content probes in four coarse-textured soil. *Appl Eng*
354 *Agric* 21(6): 999–1008. <https://doi.org/10.13031/trans.58.10761>.

355 Jiang S, Li D, Cao Z, Zhou C, Phoon K (2015) Efficient System Reliability Analysis of Slope
356 Stability in Spatially Variable Soils Using Monte Carlo Simulation. *J Geotech Geoenviron*
357 *Eng* 141(2):04014096. [https://doi.org/10.1061/\(ASCE\)GT.1943-5606.0001227](https://doi.org/10.1061/(ASCE)GT.1943-5606.0001227).

358 Kim M-I, Chae B-G, Nishigaki M (2008) Evaluation of geotechnical properties of saturated
359 soil using dielectric responses. *Geosci J* 12(1):83–93. [https://doi.org/10.1007/s12303-008-](https://doi.org/10.1007/s12303-008-0010-0)
360 [0010-0](https://doi.org/10.1007/s12303-008-0010-0).

361 Kizito F, Campbell CS, Campbell GS, Cobos DR, Teare BL, Carter B, Hopmans JW (2008)
362 Frequency, electrical conductivity and temperature analysis of a low-cost capacitance soil
363 moisture sensor. *J Hydrol* 352:367-378. <https://doi.org/10.1016/j.jhydrol.2008.01.021>.

364 Lu N, Godt JW (2008) Infinite slope stability under steady unsaturated seepage conditions.
365 *Water Resources Research* 44: W11404. <https://doi.org/10.1029/2008WR006976>.

366 Lu N, Likos WJ (2004) *Unsaturated Soil Mechanics*. John Wiley, Hoboken, N. J. 556 pp.

367 Lu N, Likos WJ (2006) Suction stress characteristic curve for unsaturated soil. *J. Geotech.*
368 *Geoenviron. Eng.* 132(2): 131–142. [https://doi.org/10.1061/\(ASCE\)1090-](https://doi.org/10.1061/(ASCE)1090-0241(2006)132:2(131))
369 [0241\(2006\)132:2\(131\)](https://doi.org/10.1061/(ASCE)1090-0241(2006)132:2(131)).

370 Mazahrih NT, Katbeh-Bader N, Evett SR, Ayars JE, Trout TJ (2008) Field Calibration
371 Accuracy and Utility of Four Down-Hole Water Content Sensors. *Vadose Zone J* 7(3):992-
372 1000. <https://doi.org/10.2136/vzj2008.0001>.

373 Morbidelli R, Corradini C, Saltalippi C, Brocca L (2012) Initial Soil Water Content as Input
374 to Field-Scale Infiltration and Surface Runoff Models. *Water Resour Manage* 26:1793–
375 1807. <https://doi.org/10.1007/s11269-012-9986-3>.

376 Muñoz-Carpena R, Shukla S, Morgan K (2005) Field Devices for Monitoring Soil Water
377 Content. Univ. of Florida, Bulletin 343, 24 pp.

378 Paltineanu IC, Starr JL (1997) Real-time soil water dynamics using multi-sensor capacitance
379 probes: laboratory calibration. *Soil Sci Soc Am J* 61:1576–1585.
380 <https://doi.org/10.2136/sssaj1997.03615995006100060006x>.

381 Polyakov V, Fares A, Ryder MH (2005) Calibration of a capacitance system for measuring
382 water content of tropical soil. *Vadose Zone J* 4:1004–1010.
383 <https://doi.org/10.2136/vzj2005.0028>.

384 Raia S, Alvioli M, Rossi M, Baum RL, Godt JW, Guzzetti F (2014) Improving predictive
385 power of physically based rainfall-induced shallow landslide models: a probabilistic
386 approach. *Geosci Model Dev* 7:495-514. <https://doi.org/10.5194/gmd-7-495-2014>.

387 Reid ME, Baum RL, LaHusen RG, Ellis WL (2008) Capturing landslide dynamics and
388 hydrologic triggers using near-real-time monitoring. In: Chen et al., (eds), *Landslides and*
389 *Engineered Slopes*. Taylor & Francis Group, London, pp. 179-191.

390 Rhoades JD, Chanduvi F, Lesch S. (1999). Soil salinity assessment: Methods and
391 interpretation of electrical conductivity measurements. *Food & Agriculture Org.* 57, 165
392 pp. Available at <http://www.fao.org/docrep/019/x2002e/x2002e.pdf>. Last accessed, July
393 31th, 2017.

394 Robinson DA, Gardner CMK, Cooper JD (1999) Measurement of relative permittivity in
395 sandy soils using TDR, capacitance and theta probes: comparison, including the effects of

396 bulk soil electrical conductivity. *Journal of Hydrology* 223:198–211.
397 [https://doi.org/10.1016/S0022-1694\(99\)00121-3](https://doi.org/10.1016/S0022-1694(99)00121-3).

398 Rossi M, Guzzetti F, Reichenbach P, Mondini AC, Peruccacci S (2010) Optimal landslide
399 susceptibility zonation based on multiple forecasts. *Geomorphology* 114(3):129-142.
400 <https://doi.org/10.1016/j.geomorph.2009.06.020>.

401 Rossi M, Reichenbach P (2016) LAND-SE: a software for statistically based landslide
402 susceptibility zonation, version 1.0. *Geosci Model Dev* 9(10):3533.
403 <https://doi.org/10.5194/gmd-9-3533-2016>.

404 Rossi M, Luciani S, Valigi D, Kirschbaum D, Brunetti MT, Peruccacci S, Guzzetti F (2017)
405 Statistical approaches for the definition of landslide rainfall thresholds and their uncertainty
406 using rain gauge and satellite data. *Geomorphology* 285:16-27.
407 <https://doi.org/10.1016/j.geomorph.2017.02.001>.

408 Rüdiger C, Western AW, Walker JP, Smith AB, Kalma JD, Willgoose GR (2010) Towards a
409 general equation for frequency domain reflectometers. *J Hydrol* 383(3):319-329.
410 <https://doi.org/10.1016/j.jhydrol.2009.12.046>.

411 Rudnick DR, Djaman K, Irmak S (2015) Performance Analysis of Capacitance and Electrical
412 Resistance-Type Soil Moisture Sensors in a Silt Loam Soil. *Transactions of the ASABE*
413 58(3):649-665. <https://doi.org/10.13031/trans.58.10761>.

414 Sahis MK, Bhattacharya G, Chowdhury R (2014) Reliability analysis of rainfall induced
415 slope instability of unsaturated soil slopes. In: N. Khalili, A. Russell & A. Khoshghalb
416 (Eds.), *Unsaturated Soils: Research & Applications*, Taylor & Francis Group, London, pp.
417 1287-1293.

418 Saxton KE, Rawls WJ (2006). Soil Water Characteristic Estimates by Texture and Organic
419 Matter for Hydrologic Solutions. Soil Sci. Soc. Am. J. 70:1569–1578.
420 <https://doi.org/10.2136/sssaj2005.0117>.

421 Saxton KE, Rawls WJ, Romberger JS, Papendick RI (1986). Estimating generalized soil
422 water characteristics from texture. Transactions of the American Society of Agricultural
423 Engineers 50:1031-1035.

424 Scudiero E, Berti A, Teatini P, Morari F (2012). Simultaneous monitoring of soil water
425 content and salinity with a low-cost capacitance-resistance probe. Sensors 12(12): 17588-
426 17607. <https://doi.org/10.3390/s121217588>.

427 Sevostianova E, Deb S, Serena M, VanLeeuwen D, Leinauer, B (2015). Accuracy of Two
428 Electromagnetic Soil Water Content Sensors in Saline Soils. Soil Science Society of
429 America Journal 79(6): 1752-1759. <https://doi.org/10.2136/sssaj2015.07.0271>.

430 Topp GC, Davis JL, Annan AP (1980) Electromagnetic determination of soil water content:
431 Measurement in coaxial transmission lines. Water Resour Res 16(3):579-582.
432 <https://doi.org/10.1029/WR016i003p00574>.

433 Van Bavel M, Nichols, C (2002) Theta and profiler soil moisture probes - Accurate
434 impedance measurement devices - New applications. Available at
435 [http://dynamax.com/images/uploads/papers/95_Theta_and_profiler_soil_moisture_probes.](http://dynamax.com/images/uploads/papers/95_Theta_and_profiler_soil_moisture_probes.pdf)
436 [pdf](http://dynamax.com/images/uploads/papers/95_Theta_and_profiler_soil_moisture_probes.pdf). Last accessed, October 19th, 2016.

437 Walker JP, Willgoose GR, Kalma JD (2004) In situ measurement of soil moisture: A
438 comparison of techniques. J Hydrol 293(1):85-99.
439 <https://doi.org/10.1016/j.jhydrol.2004.01.008>.

440 Wolle CM, Hachich W (1989) Rain-induced landslides in southeastern Brazil in, Proc. of the
441 12th Int. Conf. on Soil Mechanics and Foundation Engineering, Rio de Janeiro, Brazil, pp.
442 1639– 1644, A.A. Balkema, Rotterdam, Netherlands.

443 Zhang LL, Zhang LM, Zhang J, Tang WH (2011) Stability analysis of rainfall induced slope
444 failure: A review. P I Civil Eng-Geotec 164 (Issue GE5): 299-316.
445 <https://doi.org/10.1680/geng.2011.164.5.299>.

446

447

448

449

450

451

452

453

454

455

456

457

458

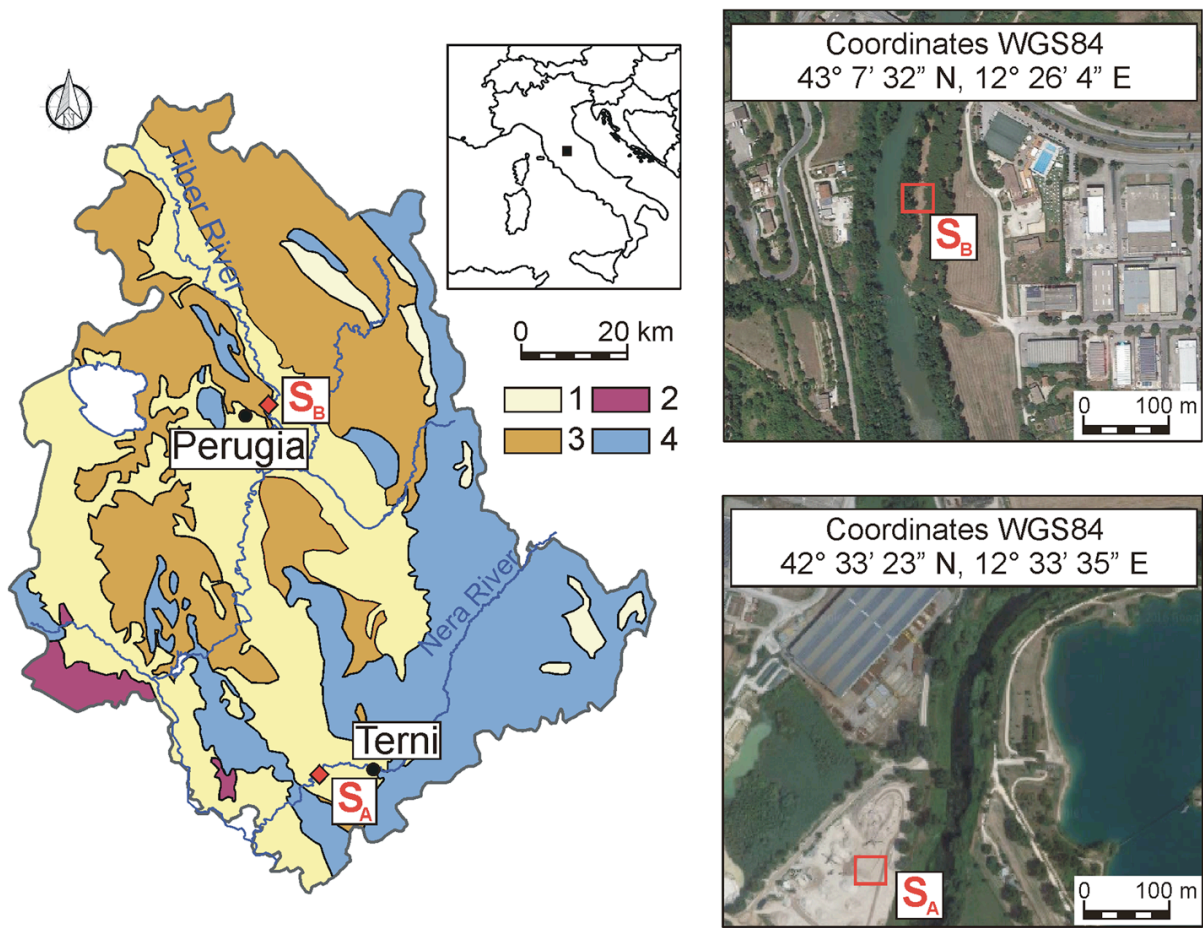
459

460

461

462

463



464
 465 **Fig. 1** Lithologic map of Umbria Region (Central Italy) with location of soil sampling sites
 466 (S_A – Conca Ternana alluvial plane – Nera River, S_B – Tiber River alluvial plane). 1) recent
 467 and ancient fluvial-lacustrine deposits; 2) volcanic deposits; 3) flyschoid rocks; 4) calcareous
 468 and marly-silici-calcareous rocks.

469
 470
 471
 472
 473
 474
 475
 476

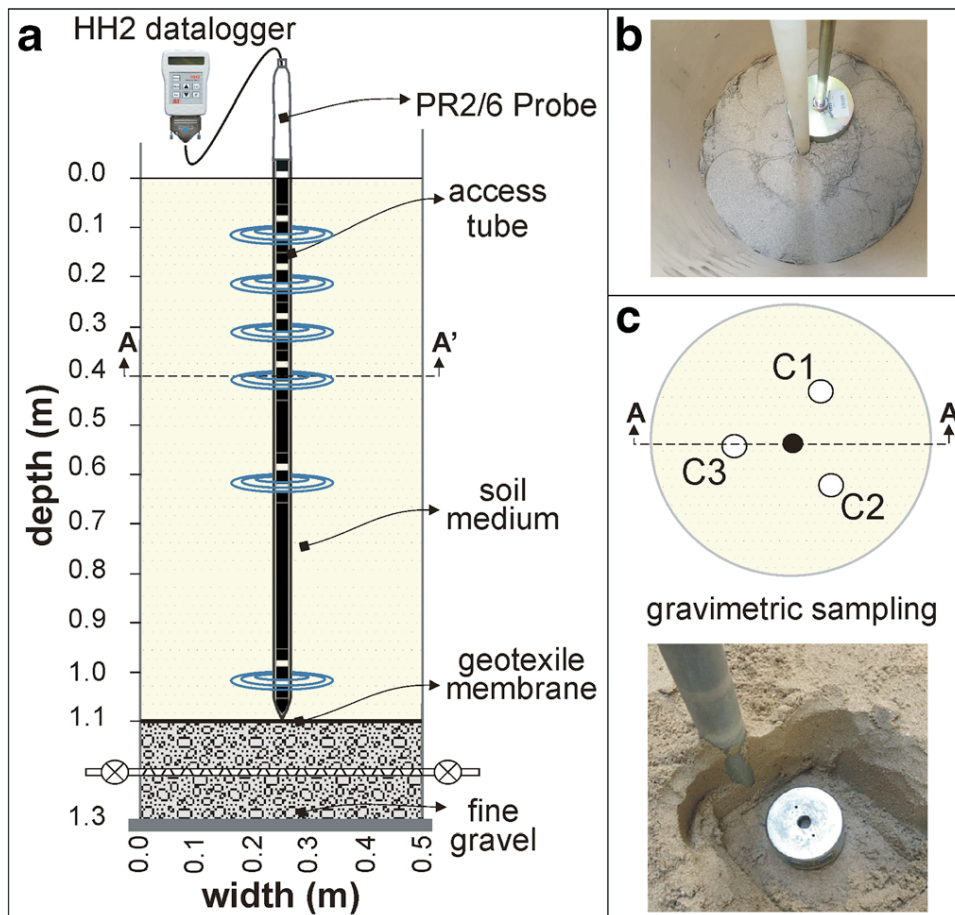
Soil	Fines	Grain size (%) Sand	Gravel	G_s	Compaction properties MDD (kN/m^3)	OMC (%)	PI (%)	OM (%)	Mineralogy
S_A	4.75	94.95	0.30	2.67	14.8	20.0	N.P.	0.37	Carbonates with subordinate minerals (muscovite, gypsum)
S_B	17.59	82.41	–	2.66	17.5	13.2	N.P.	1.53	Quartz, biotite, muscovite, pyrite, biotite, carbonaceous frustules

477

478 **Table 1** – Geotechnical e mineralogical properties of soils. G_s – specific gravity; MDD –

479 Maximum Dry Density; OMC – Optimum Moisture Content; OM – Organic Matter.

480



481

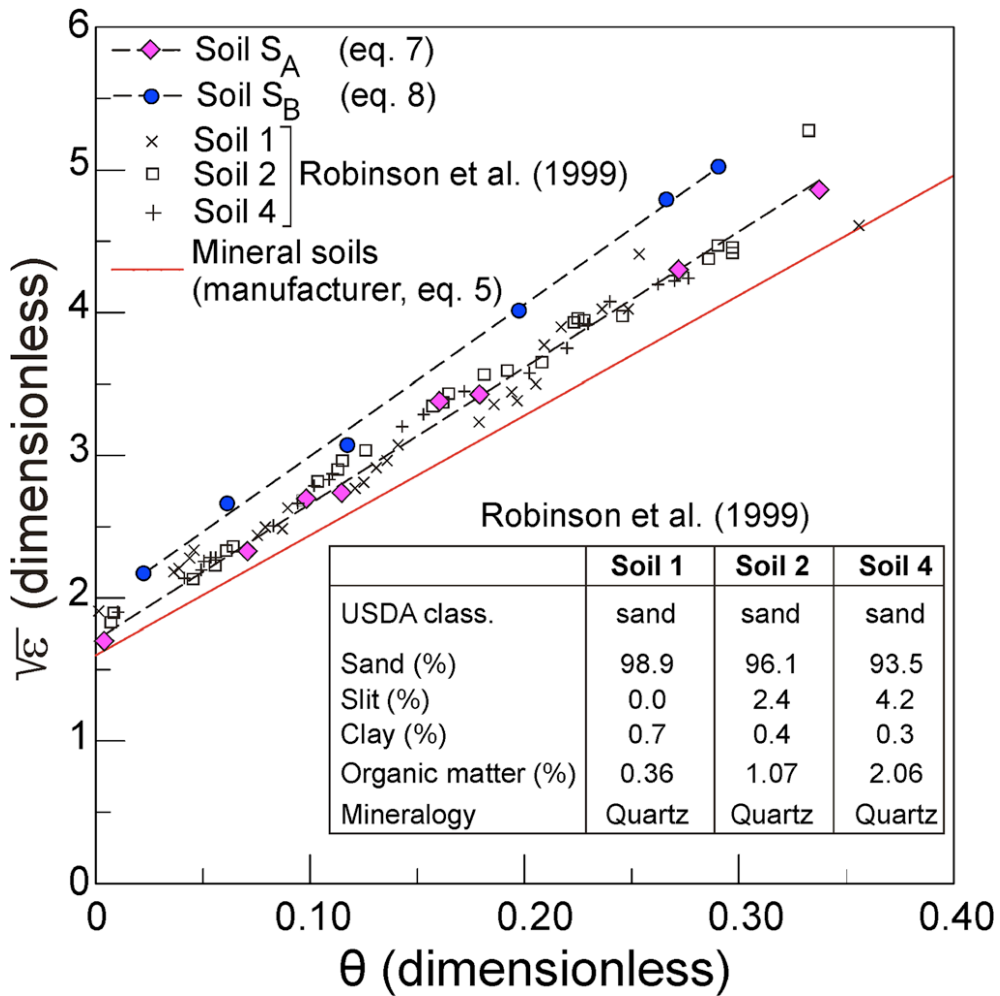
482 **Fig. 2** a) Soil column (not to scale) used to calibrate the PR2/6 probe; b) Detail of

483 compaction procedure; c) Gravimetric sampling for the measurements of θ_g used to calculate

484 θ values by eq. 3.

485

486



487

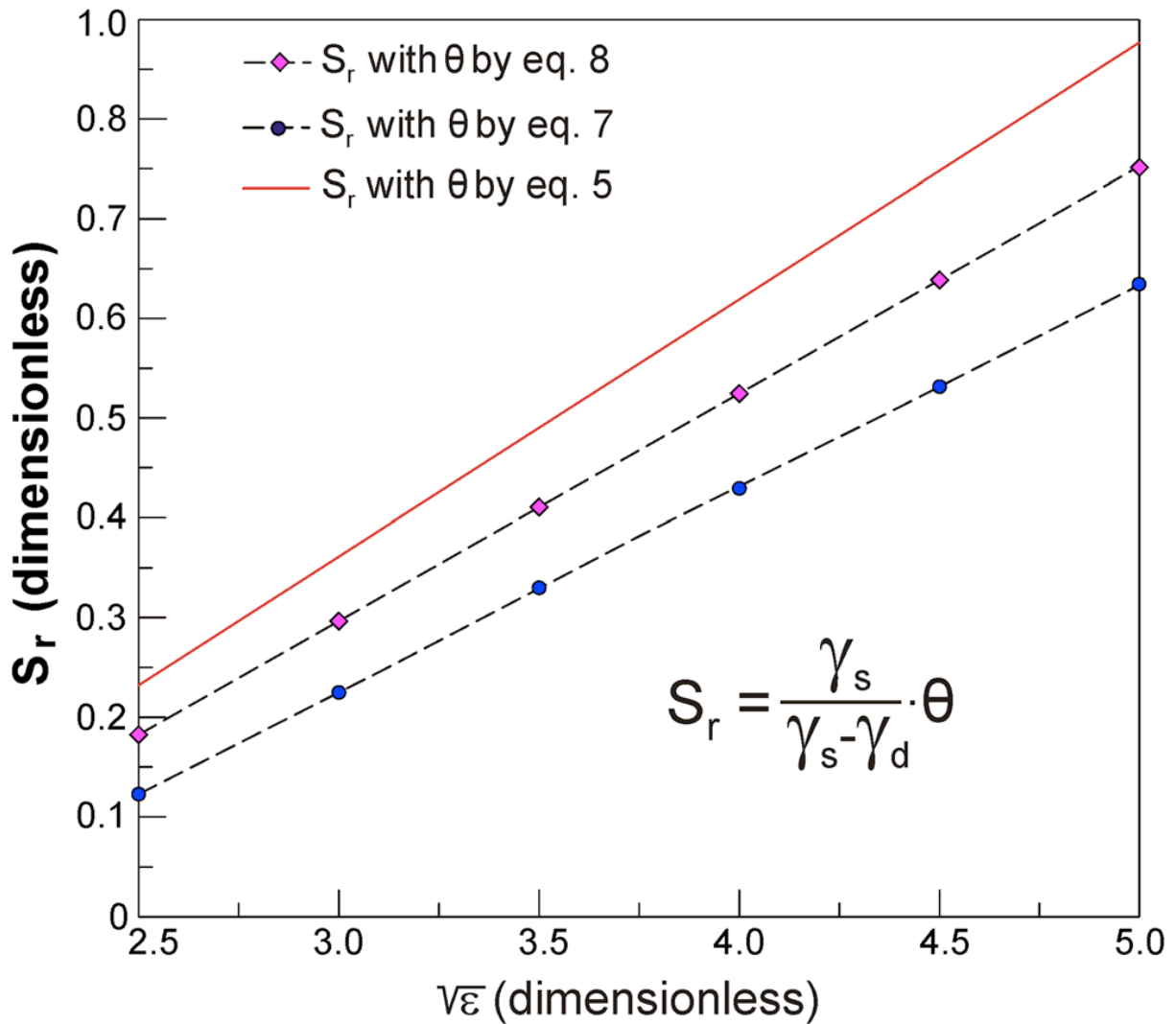
488 **Fig. 3** Laboratory relationship between the square root of dielectric constant - as measured by
 489 PR2/6 probe - and θ values obtained by soil sampling (Fig. 3c). Data are compared with
 490 those obtained with Theta probe (based on same principles of PR2/6 device) on quartz sands
 491 by Robinson et al. (1999).

Soil	θ_r	θ_s	SWCC properties		σ^s (kPa)		
			θ by eqs. 7 or 8 (calibration equations)	$u_a - u_w$ (kPa)	θ by eq. 9 (manufacturer equation)	Using SWCC properties and θ from calibration equations	Using SWCC properties and θ from manufacturer equation
S_A	0.032	0.451	18 ($\theta = 0.25$)		9 ($\theta = 0.35$)	- 8.67	- 6.74
S_B	0.033	0.452	15 ($\theta = 0.29$)			- 9.41	

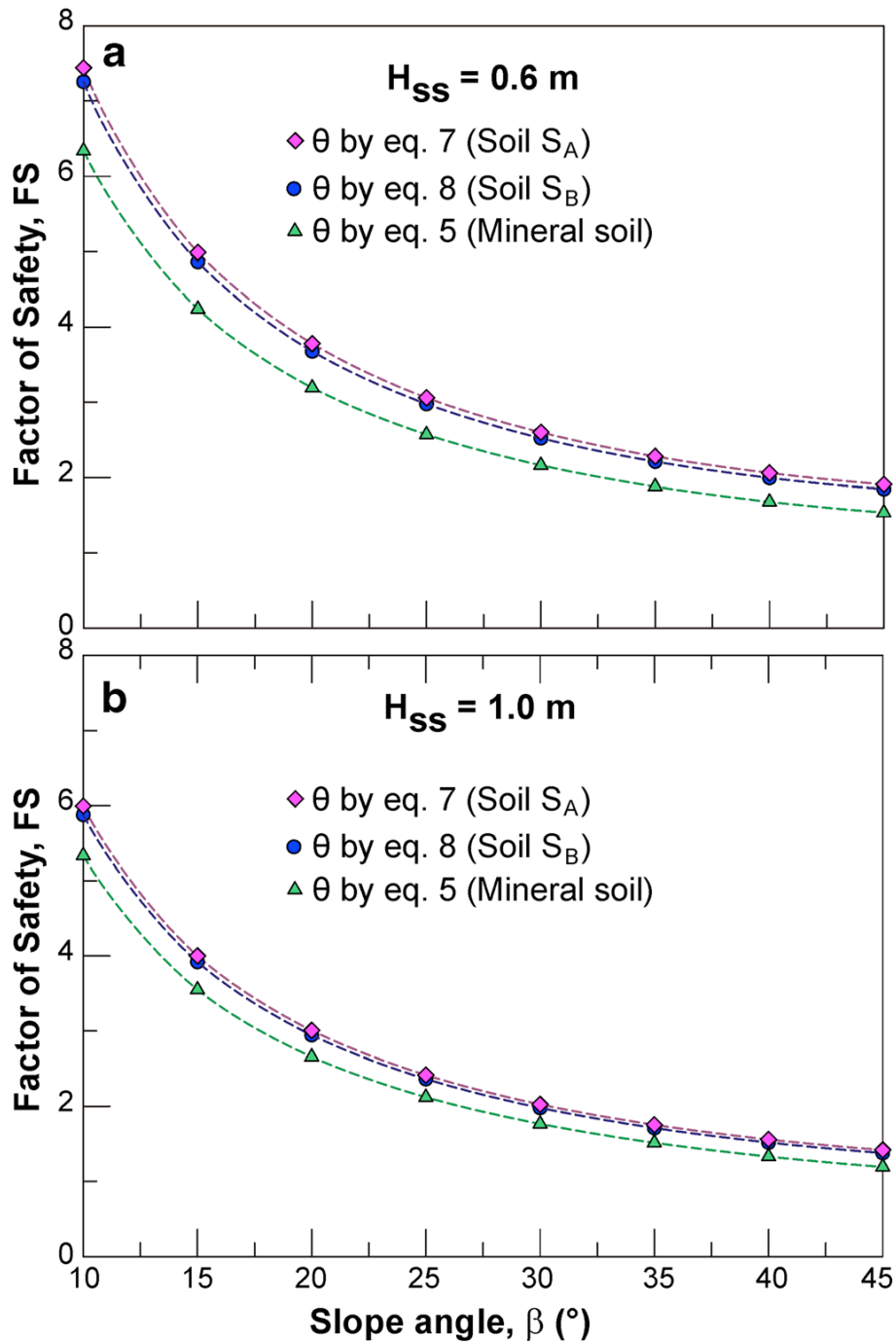
492

493 **Table 2** SWCC parameters estimated for S_A and S_B by the Saxton et al. (1986) model and
 494 suction stress values according to eq. 9.

495



499 **Fig. 4** Relationship between the degree of saturation (S_r) and square root of dielectric
 500 constant ($\sqrt{\epsilon}$) measured by PR2/6 probe. Values are calculated by considering $\gamma_d = 14.0$
 501 kN/m^3 , $\gamma_s = 26.0 \text{ kN/m}^3$, and θ computed by using the specific soil calibration (eqs. 7-8) and
 502 the generalized equation by manufacturer (eq. 5).



507

508 **Fig. 5** FS values computed by eq. 9 as a function of slope angle. Values are calculated by
 509 considering $\gamma_d = 14.0 \text{ kN/m}^3$, $\gamma_s = 26.0 \text{ kN/m}^3$, $\phi' = 34^\circ$ and $\sqrt{\epsilon} = 4.5$. a) depth of sliding
 510 surface (H_{ss}) equal to 0.6 m; b) depth of sliding surface (H_{ss}) equal to 1.0 m.